Lehigh University
Lehigh Preserve

Theses and Dissertations

1963

Stacking faults in epitaxial silicon thin films

Michael H. Notis
Lehigh University

Follow this and additional works at: https://preserve.lehigh.edu/etd

Part of the Materials Science and Engineering Commons

Recommended Citation
Notis, Michael H., "Stacking faults in epitaxial silicon thin films" (1963). *Theses and Dissertations*. 3158.
https://preserve.lehigh.edu/etd/3158

This Thesis is brought to you for free and open access by Lehigh Preserve. It has been accepted for inclusion in Theses and Dissertations by an authorized administrator of Lehigh Preserve. For more information, please contact preserve@lehigh.edu.

STACKING FAULTS IN EPITAXIAL SILICON THIN FILMS

by

Michael Richard Notis

A Thesis

Presented to the Graduate Faculty

of Lehigh University

in Candidacy for the Degree of

Master of Science

Lehigh University

1963

This thesis is accepted and approved in partial fulfillment of the requirements for the degree of Master of Science.

Sept 18, 1963
(Date)

George P. Conard III
Professor in Charge

Head of the Department

Acknowledgements

I wish to express my appreciation to the Western Electric Company for providing the facilities for the work done in this thesis. In particular, I would like to thank Messrs. J. C. Yastrzab and E. J. Saukulak for their help in preparing the epitaxial slices, T. F. Briody for helpful advice, G. P. Conard, III, of Lehigh University, R. J. Jaccodine and R. E. Caffrey of Bell Telephone Laboratories for many rewarding discussions. I am grateful to Mrs. A. B. Schock for her help in typing and preparing the final copy from my original notes. Lastly, I am more than indebted to the consideration and encouragement of my wife, Ruth, who was instrumental in insuring the completion of this work.

TABLE OF CONTENTS

Page Number

Abstract 1

1.0 Theory of Vapor Growth 2

1.1 Introduction 2

1.2 Phenomonological Approach to Equilibrium Growth 3

1.3 Atomic Approach to Growth Kinetics 5

1.4 Epitaxial Growth 8

2.0 Imperfections in Epitaxial Films 13

2.1 Introduction 13

2.2 Growth Pyramids in Epitaxial Films 14

2.3 Dislocations in Epitaxial Films 15

2.4 Stacking Faults 17

2.4.1 General Stacking Fault Theory 17

2.4.2 Stacking Faults in Epitaxial Films 20

3.0 Experimental 24

3.1 Scope 24

3.2 Growth of Epitaxial Silicon Films 25

3.3 Substrate Preparation and Cleaning 28

3.4 Observation of Imperfections on Silicon Films 30

3.5 Results 31

3.5.1 Dislocations in the Layers vs. Dislocations in the Substrate 31

3.5.2 Stacking Faults in the Layer vs. Dislocations in the Substrate 33

Page Number

3.5.3 Stacking Faults vs. Growth Rate 35

3.5.4 Stacking Fault Density vs. Substrate Dislocation Density 37

3.5.5 Stacking Faults vs. Preparation and Cleaning Procedures 38

3.6 Conslusions and Discussion 39

4.0 Appendix A - Interference Contrast Microscopy 42

5.0 Appendix B - Infrared Interference Thickness Measurement 44

6.0 Bibliography 46

7.0 Figures 49

Figure 1 - Diagramatic Illustration of the Experimental Epitaxial Deposition System 50

Figure 2 - Relationship Between Time and Pit Density for Silicon Epitaxial Layers Etched in Dash Etch 52

Figure 3 - Overlay Pattern Showing the Relation of Dislocation Pits in the Substrate to Dislocation Pits in the Layer 54

Figure 4 - Overlay Pattern Showing the Relation of Dislocation Pits in the Substrate to Stacking Faults in the Layer 56

Figure 5 - Relationship Between Growth Rate and Stacking Fault Density 58

Page Number

Figure 6 - Relationship Between Substrate Dislocation Density and Stacking Fault Density in the Layer 60

Figure 7 - Relationship Between Incident and Reflected Beams for the Infrared Measurement of Epitaxial Thickness 62

8.0 Plates 64

Plate 1 - Interference Fringes on a Flat Epitaxial Deposit. 200x. 65

Plate 2 - Interference Fringes on an Epitaxial Layer Showing Pitting. 200x. 67

Plate 3 - Etch Pits in Epitaxial Silicon Layers Etched in Dash Etch for 4 Hours. 500x. 69

Plate 4 - Stacking Faults in Epitaxial Silicon Layer Etched in CP-4 for 4 seconds. 200x. 71

Plate 5 - Stacking Faults in Epitaxial Silicon Layer Etched in CP-4 for 2 Minutes. 200x. 73

Plate 6 - Stacking Faults in Epitaxial Silicon Layer Etched in CP-4 for 4 Minutes. 200x. 75

Plate 7 - Stacking Fault in Epitaxial Silicon Observed by Interference Contrast Microscopy. 200x. 77

Plate 8 - Growth Pyramid Showing Steps on Epitaxial Silicon Layer Grown at 0.1 Micron per Minute. 1000x. 79

Page Number

9.0 Tables 81

Table 1 - Comparison of Layer Thickness Values Calculated From Fault Edge and Infrared Techniques 82

Table 2 - Radial Variation of Stacking Fault Density 83

Table 3 - Comparison of Preparation Techniques on Stacking Fault Density 84

10.0 Biography 85

ABSTRACT

A review of the literature involving growth from the vapor and epitaxial growth up to August 1963 is presented. Next, experimental results of the effects of growth rate, substrate perfection and cleanliness are presented. Lastly, some consideration is given to the mechanism by which stacking faults are formed in epitaxial silicon thin films.

It is proposed that stacking faults are generated by the collapse of vacancy clusters as a natural consequence of the low stacking fault energy. Experimental evidence showing the effect of growth rate and substrate dislocation density on stacking fault density is presented to support this view.

1.0 THEORY OF VAPOR GROWTH

1.1 INTRODUCTION

The theory of crystal growth has developed simultaneously from two related fields. The phenomonologists have developed the theory of equilibrium between a crystal and the medium in which it grows from a classical Gibbsian thermodynamic picture, while the atomists have interpreted the kinetics of a growth process from a consideration of atomic structure and statistical mechanical methods. Any attempt to review the historical development of crystal growth would necessarily be divided in a similar manner.

1.2 PHENOMONOLOGICAL APPROACH TO EQUILIBRIUM GROWTH

In 1878, J. W. Gibbs (1) proposed a thermodynamic approach to equilibrium situations which has since spurred many areas of endeavor and has caused major advances in the field of crystal growth. A consideration of surface energy and knowledge of simple nearest atomic neighbor relationships enables one to draw conclusions about the orientation and structure of bounding crystal surfaces. This approach was developed by Curie (2) and Wulff (3) who proposed that, "If a body is in its equilibrium shape, there exists a point whose perpendicular distance from every face is proportional to the surface free energy of that face". The proportionality constant was found to be given by the Gibbs-Thomson equation for the dependence of vapor pressure on size of spherical droplets, which may be written as:

$$\frac{\nu_1}{h_1} = \frac{\nu_2}{h_2} = \frac{kT}{2\Omega} \ln \frac{P}{P_o}$$

Where h = normal distance

ν = surface energy

Ω = volume per molecule

P = actual vapor pressure

P_o = equilibrium vapor pressure

Indeed, Wulff developed a construction for deriving the equilibrium shape of a crystal from a polar diagram of surface free energy as a function of crystal orientation. The proposals

formed by Curie and Wulff were proved by Hilton (4) in 1903. This work has recently been extended and reformulated by Herring (5) who has proposed a well founded relationship between the equilibrium shape of a crystal and its surface energy and chemical potential, which he used to discuss the stability of a crystal surface upon thermal etching. In this manner, corollaries have been added to the original theorem and may be stated as follows:

(1) The faces of low surface free energy tend to be faces of low growth rate.

(2) The orientation of these faces naturally correspond exactly since they are faces of low index.

Curie assumes that, under ideal controlled conditions, crystals would form in their equilibrium shape; but a closer look at the Gibbs-Thomson equation points out that the shape dependence of free energy is inversely proportional to size. Frank (6) pointed out that, for crystals larger than a micron in size, the deduction of shape from the above considerations loses its validity. Thus, in actuality, these surface energy equilibrium forms are not experimentally obtained because of the strong dependence of form on growth rate and dissolution rate as a function of crystallographic orientation. A combined approach to the problem has been made by Batterman (7) and Jaccodine (8) whose experimental work with germanium and gallium arsenide agree quite well with predictions.

1.3 ATOMIC APPROACH TO GROWTH KINETICS

The kinetic approach to the growth problem maintains as its starting assumptions that the growth of a crystal from the vapor is carried out by the nucleation of small areas of monolayers, and that the completion of growth on that surface is by the extension of the monolayer areas. This nucleation process was first recognized by Gibbs (9). Any finite monolayer area must have a higher vapor pressure than the infinite crystal, and this increased vapor pressure is caused by the specific free energy of the monolayer edge. It may be shown (10) that, for a given degree of supersaturation, there is a critical nucleus size (R_c) for which the monolayer is in unstable equilibrium. This critical nucleus size may be expressed as:

$$R_c = aE_e \left[kT \ln\alpha\right]^{-1}$$

Where a = material constant related to molecular volume

E_e = monolayer edge energy per atom

α = ratio of vapor pressure (P) to equilibrium vapor pressure (Po)

Thus, if the nucleus formed is greater than R_c, the monolayer will grow; if the nucleus is smaller than R_c, the monolayer will evaporate.

The rate of formation of critical nuclei has been shown to be given (11) as:

$$N = A\left(\frac{S}{S_A}\right) \exp\left[\frac{-4E_e^2}{k^2T^2\ln\alpha}\right]$$

Where N = rate of formation of critical nuclei

A = rate of arrival of new atoms at a single surface lattice site

S = surface area of crystal face

S_A = surface area per atom of the crystal face.

Volmer (12) has calculated the supersaturation required to produce an appreciable growth rate to be not less than 25%. Experimental evidence, however, has shown very few systems to be in agreement with the expectations of this surface nucleation theory (13). Volmer and Schultz (14) studied the growth rate of Iodine crystals and found that, for supersaturations above 1%, the growth rate was proportional to the supersaturation.

In order to explain the experimental divergencies from theory, Frank (15) proposed a theory of growth of imperfect crystals. The Frank theory proposed that, because crystals were not ideal in nature but contained imperfect or dislocated areas, these imperfections would act as sources of enhanced growth. In particular, Frank proposed that a screw dislocation (one whose slip vector is parallel to the dislocation axis) which met a crystal surface at a right angle would provide a monolayer step for the continuation of crystal growth and eliminate the need for nucleation processes because the dislocated crystal could be pictured as a dislocated monolayer. As atoms are added to the monolayer step, the step advances in a spiral path along the axis of the dislocation. The velocity with which any section of the step advances is proportional to the supersaturation of the vapor which, in turn, decreases with

local curvature. As the spiral grows, the section nearest the dislocation achieves a higher curvature and thus an increase in local equilibrium vapor pressure. Finally a steady state condition is reached in which the angular velocity is the same for all points on the step and the shape remains unchanged. The theory was enlarged and given quantitative form by Burton and Cabrera (16) and by Burton, Cabrera and Frank (17). The Frank theory was immediately accepted and experimental proof was forthcoming before the theory had been completely formalized. Amelinckx (18) observed Frank sources in gold, Forty (19) in magnesium and cadmium iodide, Griffin (20) in natural beryl, Dawson and Vand (21) in paraffin, and Verma and Amelinckx (22) in silicon carbide. Since this time, an effort has been made to unify the general field of vapor growth by a joint approach of phenomonology, atomic structure and statistical mechanics (23), and has greatly modified previous concepts of two dimensional nucleation and dislocation propagated growth mechanisms. Even with this new approach, a more general basis must be established via irreversible thermodynamics because of the transient nature of most crystal growth experiments. In addition, particular studies have been carried out in the fields of growth theory of filamentary whiskers (24), mathematical approaches to vapor growth (25), and epitaxial growth.

1.4 EPITAXIAL GROWTH

In 1925, VanArkel (26) showed that solids can be crystallized from a gaseous as well as a liquid phase through his work on the deposition of tungsten from the gaseous hexachloride. The economic importance of this discovery immediately dictated an experimental effort which has lasted to the present day. Many investigators noted a crystallographic orientation relation between these vapor deposited metals and their substrates, but it was not until 1928 when Royer (27) defined the general system. He defined epitaxial growth as the growth of a crystal upon another crystal with a related structure whereby the orientation of the deposit has a fixed and rigid relation to the substrate. Royer provided the first set of rules for epitaxial growth depending on the per cent mismatch between the two lattice systems. From that time until the late Forties, much experimental work was done to show that oriented metal films could be vacuum-deposited on a variety of single crystal substrates (28), but it was not until the imperfect nature of crystal structure was noted that extensive advances were made in theory.

In 1949, Frank and Van der Merwe (29) developed the theory for a one-dimensional dislocation model which was applied to the growth of monolayers on a crystalline substrate. They applied this model to the case of a monolayer on the surface of a crystalline substrate with different lattice spacing and showed how faulting

of the layer could provide an oriented overgrowth of a misfit monolayer. The misfit rules proposed by Royer limited the systems to very small mismatch, but the Frank - Van der Merwe Theory explained how systems with large mismatch could extend over macroscopic distances if dislocations with suitable Burgers vector are introduced to relieve the internal stress of the system. Experimental results of the past were reviewed (30,31) in an effort to revise Royer's Misfit Rules in the light of the imperfect nature of growth, but many questions were still left unanswered.

Deo, Finch and Gharpurey (32), when working with the epitaxial systems of methylene blue and NH_4I on cleaved mica surfaces, noted that the epitaxial growth of the system depends only on the first few deposited atom layers, and that further growth is no longer affected by the substrate lattice structure. They found that the deposited crystal size was uniform over the layer and suggested that, when a certain degree of supersaturation is attained, nuclei are formed simultaneously at a number of positions on the surface. Further deposition is confined to these initial nuclei, and subsequent growth is independent of substrate structure.

Blisnakov (33) proposed a thermodynamic explanation for the critical temperature at which epitaxy was observed to appear between two crystalline phases. He derived an expression for Δa_{max} (the largest difference between lattice constants of the deposit and substrate at which epitaxy between given planes can occur) in terms of elasticity coefficients, work of removal and deformation of

crystal nuclei, surface concentration and substrate temperature. An epitaxial deposit would thus be obtained if the system was designed so that $\Delta a \leq \Delta a_{max}$. Baur (34) extended Blisnakov's work and showed that crystal growth atom-layer by atom-layer through surface nucleation (Frank - Van der Merwe mechanism) can occur only for growth systems where both deposit and substrate are of the same component. For multi-component systems, growth could occur by either of two mechanisms:

(1) Stranski - Krasnov Mechanism whereby the original formation of a unimolecular or multimolecular layer occurs without nucleation and then leads to the formation of three dimensional nuclei, or

(2) Volmer - Weber Mechanism where three dimensional nuclei are formed directly on the foreign substrate.

Based on the above mechanisms and the probability of nucleation, Baur then discusses the conditions under which epitaxial growth will occur. Other attempts at a reasonable theory for epitaxial growth include Dixit's (35) application of a two-dimensional gas theory for the growth of thin metal films to epitaxial growth by introducing a Van der Waal's force depending on the attraction between substrate ions and deposited atoms. He considers both the deposition of neutral atoms from solution and by electrolytic deposition.

Recently, work has been done by Pashley (36) with the evaporation of gold and silver on cleaved mica or halide substrates

inside an electron microscope which revealed that small discrete nuclei are formed and not a thin monolayer. As these nuclei grow, then tend to coalesce, the smaller ones being attracted to the larger ones. Pashley terms this "atomic migration".

In 1960, germanium was deposited epitaxially on germanium substrates (37), and in 1961, silicon was deposited in a similar manner (38). These semiconductor epitaxial films provided material for solid-state electronic applications (39) which yielded devices with extremely low collector-emitter saturation voltages and high breakdown voltages. Kurov (40) developed a mechanism to explain the germanium epitaxial system by applying the theory for the rate of formation of two-dimensional nuclei proposed by Burton, Cabrera and Frank (17). He took into consideration four means by which the degree of structural perfection of the epitaxial layer could be affected:

(1) The degree of structural perfection of the substrate

(2) Surface films and adsorbed layers on the substrate surface

(3) Impurity atoms present in both the vapor and substrate

(4) The degree of departure from thermodynamic equilibrium of the system during growth.

On the basis of the above factors, Kurov proposed a system whereby almost every atom incident upon the substrate surface remains and migrates upon it. As a result of this migration, a number of nuclei are formed, each consisting of a few atoms and the growth of the layer begins simultaneously at many points on

the substrate. Because the rate of supply of atoms is greater than the rate at which new layers are nucleated, many incomplete layers are nucleated simultaneously. Under conditions such as these, where growth has deviated far from equilibrium conditions, the formation of a large number of defects is shown to be possible.

2.0 IMPERFECTIONS IN EPITAXIAL FILMS

2.1 INTRODUCTION

The realization that epitaxial devices offer much improved design characteristics to electronic producers created a situation where epitaxial growth was viewed as a production method for the first time. Rigorous investigation showed these films to be highly imperfect for production use and a surge of investigation of imperfections in epitaxial films was started. Until this time, little work had been attempted in this field. Vermout and Dekeyser (41), working with oriented overgrowths of silver on cleaved substrates of rock salt, made passing reference to the possibility that imperfection of the substrate surface might play a more important role than previously considered.

Imperfections found to be present in epitaxial films of germanium and silicon may be classed into three groups:

(1) Growth Pyramids

(2) Dislocations

(3) Stacking Faults

Experiment and advances in technology tend to show that imperfections except stacking faults are introduced almost exclusively by the failure to produce a clean or properly oriented system.

2.2 GROWTH PYRAMIDS IN EPITAXIAL FILMS

Ingham and McDade (42) and Ingham, McDade and Compton (43) noted growth pyramids in germanium epitaxial films and suggested that they were formed by the enhanced growth around a screw dislocation emerging at the substrate surface. Light (44) and Reizman and Basseches (45) noted the appearance of pyramids in silicon epitaxial films. Chu and Gavaler (46) cite work done by themselves on silicon and by Ingham and McDade (42) on germanium which show that substrates oriented a few degrees off of major crystallographic planes do not show growth pyramids, but still propose that the probable cause of pyramid formation is an impurity effect. Flint, Lawrence and Tucker (47) noted the presence of growth pyramids in silicon films grown by the vapor deposition of trichlorosilane in hydrogen atmospheres and have associated them with the presence of stacking faults.

Recent work by Tung (48) and Edmunds and Gibson (49) shows that surface defects of the growth pyramid type are a function of (1) growth rate and (2) substrate orientation. These pyramidal defects were not observed when the growth rate was less than 2.5 microns per minute and misorientation was greater than one-half degree off the $\{111\}$ crystallographic planes. It is thus proposed (50) that orientations slightly off a major crystallographic plane provide an increased number of surface steps which produce sites for easy nucleation.

2.3 DISLOCATION IN EPITAXIAL FILMS

The observation of dislocations in epitaxial films is by no means a recent development. As mentioned previously, Frank and Van der Merwe (29) proposed a theory for epitaxial growth based on the action of dislocations at the growth interface. Since that time, many reviews and books have been written (51,52,53) on the geometrical description and properties of dislocations so they shall not be dwelled upon here.

Ingham and McDade (42) reported the presence of dislocations in epitaxial germanium films grown onto substrates during the disproportionation of GeI_2 to Ge and GeI_4 (37). In this work, substrates were (111) oriented germanium wafers and they were sectioned after growth so that etch pit densities could be observed across the junction of deposit and substrate in the $\langle 11\bar{1} \rangle$ direction. It was found that dislocation densities decreased on either side of the interface, and that the perfection of the layer is largely controlled by the substrate surface condition. Ingham, McDade and Compton (43) demonstrated that, in germanium epitaxial systems, dislocations may originate in the deposit as well as by propogation from the substrate. The findings of Beatty, Glang and Kren (54) and Glang and Wajda (55) in the silicon epitaxial system indicate good agreement with those for the Ge system. They note a strong dependence of dislocation density in the layer on substrate preparation, but also observe a high variation of dislocation density

at the substrate edge. This density increase is attributed to inherently greater temperature variations at the slice edge and is in agreement with the theory of dislocation generation by the application of thermal gradients as proposed by Dash (56).

Chu and Gavaler (46) duplicated the work of Ingham and McDade (42) and Ingham, McDade and Compton (43) for the silicon epitaxial system and the results were found to be substantially similar. It is explained that dislocations present at the interface may be introduced by the indiffusion of small diameter impurity atoms from the substrate. Substitutional impurity atoms would contract the lattice (57) and set up stresses capable of generating dislocations.

Refinements in epitaxial growing techniques, proper cleanliness, and well designed systems have reduced the importance of dislocations and growth pyramids. The problem of stacking faults, however, has not been resolved and their effect on semiconductor device parameters has not been clarified.

2.4 STACKING FAULTS

2.4.1 GENERAL STACKING FAULT THEORY

A stacking fault may be defined (58) as an interruption in the atomic stacking sequence of a crystal lattice which still maintains true nearest neighbor and number relationships. Heidenreich and Shockley (59) proposed the generation of stacking faults by the dissociation of a dislocation into partials. The application of Frank's Energy Rule (60) to the reaction

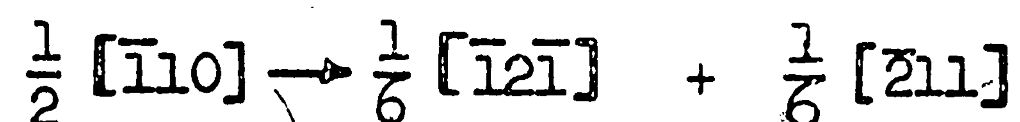

$$\frac{1}{2}[\bar{1}10] \rightarrow \frac{1}{6}[\bar{1}2\bar{1}] + \frac{1}{6}[\bar{2}11]$$

shows a reduction of energy to the right, and as the partials separate a low energy stacking fault boundary is formed in the slip plane between them. The fault energy just balances the repulsive force between the dislocations at some critical distance (51) Γ, given by:

$$\Gamma = \mu a^2/24\pi\epsilon$$

Where μ = Shear modulus

a = Lattice constant

ϵ = Fault energy per unit area

The geometry and reactions of partial dislocations which produce stacking faults has been covered quite extensively in the literature (52,53). Because the formation of a stacking fault depends upon its energy, this question has also been a source of great activity. Heidenreich and Shockley (59) related the stacking fault energy in cobalt to the energy of transition from face-centered cubic structure to hexagonal close-packed structure.

They estimated this stacking fault energy to be of the order of 20 $erg \cdot cm^{-2}$.

Seeger and Schoeck (61) proposed that stacking faults in face-centered cubic materials may be considered as thin sections bounded by coherent (111) twin boundaries. Using this principle and work performed by Fullman (60) on the measurement of twin boundary energies in Cu and Al, they calculate the stacking fault energy of Cu to be 40 $erg \cdot cm^{-2}$ and that of Al to be 200 $erg \cdot cm^{-2}$. It was suggested by Seeger (58) that, in hexagonal close packed structures, the grain-boundary energy of a low angle grain boundary composed of extended dislocations should depend on the stacking fault energy. He also proposed a qualitative approach based on electron theory. Thus low valency elements, such as Cu, Ag, Au would have low stacking fault energies because the conduction electron energies are not highly influenced by position of zone boundaries, while multivalent metals such as Al, Mg, Zn, and Cd would be expected to have high stacking fault energies because of the overlap of conduction electrons with the first Brillouin Zone. Later work (62) indicates that the activation energy for cross-slip of a pair of extended dislocations is related to stacking fault energy.

Experimental work performed by Hirsch and Silcox (63) and Silcox and Hirsch (64) shows the presence of stacking faults in quenched gold samples. These stacking faults are attributed to the collapse of vacancy discs into dislocation loops composed of

sessile Frank partial dislocations bounded by stacking faults in low stacking fault energy materials. Aluminum samples prepared in the same manner show no evidence of stacking faults. The authors point out that, in high stacking fault energy materials, the stacking fault is not a stable configuration and would be eliminated by the reaction of the Frank sessile with a Shockley partial. This reaction is given by Kuhlman-Wilsdorf (65) as:

Nakayama, Weissman and Imura (66) have recently noted the presence of stacking faults in tungsten, and Howie (67) has noted them in Cu-7%Al alloys.

2.4.2 STACKING FAULTS IN EPITAXIAL FILMS

The investigation of the nature and cause of stacking faults in epitaxial films has been the subject of many recent papers. Sloope and Tiller (68) reported on the effects of environmental conditions on the structural perfection of epitaxial single crystal silver films on sodium chloride substrates. Their results indicate a rate dependent minimum deposition temperature for the formation of single crystal films; and the structural perfection, porosity and stacking fault density of the films are found to be related to deposition rate, deposition temperature and film thickness.

Semiconductor epitaxial thin films have been studied by three main methods. Various authors have investigated the nature of these imperfections by either chemical etching (54,44), X-ray diffraction microscopy (69,70), or electron transmission microscopy (71,72).

Beatty, Glang and Kren (54) have observed imperfections in silicon epitaxial layers by etching for four hours in an etch consisting of:

30 ml HF

15 ml HNO_3

1.1 grams $Cu(NO_3)_2$

0.1 ml Br

450 ml H_2O

They have noted the formation of dark triangular pits whose etching characteristics suggest stacking faults. Light (44) has revealed triangular pits with flat centers, by etching for 30 seconds in the Westinghouse silver etch (73), which are identified as stacking faults in both germanium and silicon. These faults are attributed to surface imperfections, and it is thus proposed that the faults are originated at the interface. Geometrical relations are given which explain the presence of line, wedge and triangle faults and the orientation of these faults is given. The author states the fault sides to be in ⟨110⟩ directions and in the (111) plane, and if the fault is pictured as a regular tetrahedron with the origin of the apex at the interface, then the film thickness should be related to the length of stacking fault on the (111) plane according to the relationship.

$$t = L \sin 54.7°$$

Comparison of thickness measurements from stacking fault size are made to those from angle lapping and staining data and are found to be in excellent agreement. Later work by Lenie (74) and Dash (75) all give support to Light's original supposition.

Schwuttke (69) has identified the etching forms noted by Light as stacking faults through the use of an X-ray diffraction technique developed by Lang (76). Schwuttke and Sils (70) have shown these stacking faults to consist of partial dislocations of Burgers vector 1/6 ⟨110⟩ when in the form of a closed triangular figure, or 1/6 ⟨112⟩ when in the form of a line. Haase (77) has

examined vacuum evaporated germanium films using transmission electron microscopy and identified the imperfections in these films as stacking faults or repeated stacking faults (microtwins) on {111} planes which intersect the deposit surface along ⟨110⟩ lines.

The conditions under which these stacking faults form have been categorized by workers in this field. Schwuttke (69) proposed that they are caused by scratches, dust particles or other impurities. Queisser, Finch and Washburn (71) group the causes into five different areas, quote:

"(1) Substrate surface damage

(2) Growth mistakes at the interface

(3) Inclusions of foreign particles in the deposit

(4) Growth faults caused by lattice mismatch of layer and substrate

(5) Condensation of vacant lattice sites".

Booker and Stickler (72) picture epitaxial growth as a nucleation and two-dimensional growth system whereby random nuclei are formed on the surface, and surface migration causes the nucleated areas to join. New layers may form before preceding layers have been completed and, by deposition in an incorrect atom sequence, geometrical stacking faults may be formed.

Finch, Queisser, Thomas and Washburn (78) propose the mechanism of fault formation to be the formation of stacking faults in order to provide coherency in the lattice when the epitaxial

material is forced to grow around a surface oxide inclusion. However, the results of Batsford and Thomas (79) contradict these findings and present data that show low stacking fault density layers formed under conditions which would promote oxide films at the interface.

3.0 EXPERIMENTAL

3.1 SCOPE

The purpose of this investigation is to:

(1) Observe imperfections in epitaxial silicon films,

(2) Observe the effect of growth rate on imperfections,

(3) Observe the effect of substrate crystallographic perfection on imperfections, and

(4) Observe the effect of substrate preparation and cleaning on imperfections.

3.2 GROWTH OF EPITAXIAL SILICON FILMS

Epitaxial silicon films were formed by the hydrogen reduction of silicon tetrachloride. This reaction was first given by Theuerer (80) as:

$$SiCl_4 + 2H_2 \longrightarrow Si + 4HCl$$

Recent identification of the presence of $SiHCl_3$ in the exit gas system has been made and an experimentally determined reaction has been given as:

$$2SiCl_4 + 3H_2 \rightleftharpoons Si + SiHCl_3 + 5HCl$$

Allegretti and Pollak (81) have proposed the component reactions to be:

$$(1)\quad 2SiCl_4 + 2H_2 \longrightarrow 2SiCl_2 + 4HCl$$

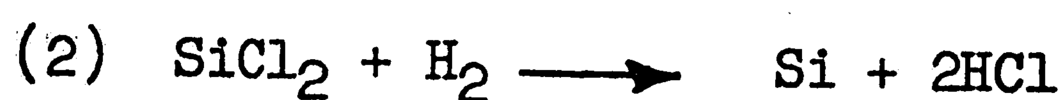

$$(2)\quad SiCl_2 + H_2 \longrightarrow Si + 2HCl$$

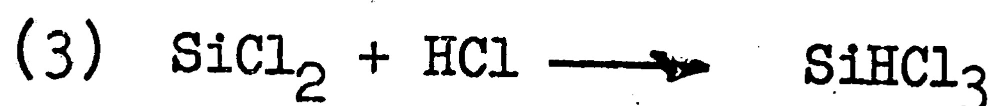

$$(3)\quad SiCl_2 + HCl \longrightarrow SiHCl_3$$

The experimental deposition system used for this investigation is shown diagramatically in Figure 1. Helium was dispensed from a regulated tank source and fed into the system at a flow rate of 10 liters per minute until the line system and the deposition chamber had been purged of air. During this operation, the bubbler was purged with helium but vented to air by opening valve A and closing valve B. After purging the system of air, hydrogen was dispensed from a regulated tank source through an automatic dual tank dryer and deoxidizing unit and then allowed to purge the entire system in the same manner as the previous

helium purge. The hydrogen purge flow rate was kept at 9 liters per minute for an elapsed purge time of 25 minutes. During this time, the temperature of the silicon tetrachloride bubbler was adjusted to +10°C±1°C by adjusting the dry ice and ethylene glycol mixture around the bubbler, and the hydrogen flow through the bubbler was adjusted to 1.5 liters per minute. This produced a gas mixture (82) of 5-6% $SiCl_4$ coming out of the bubbler, or about 2% when mixed with the bypass gas.

After the completion of the hydrogen purge, the generator power was turned on and the system was brought up to a temperature of 1150°C±5°C and held for a high-temperature bakeout in hydrogen for 5 minutes before closing valve A and opening valve B and allowing deposition to occur. Deposition rates of 0.7 to 1.2 microns per minute were achieved in either of the two deposition chambers.

The horizontal chamber consisted of a 4 inch diameter quartz tube encompassed by the element coils of the generator. The silicon substrates were placed on a graphite pedestal which, in turn, was placed inside the chamber. Carrier gas containing silicon tetrachloride was allowed to enter the chamber at one end of the quartz tube.

The vertical system was composed of a quartz bell jar assembly which contained the pedestal system. The silicon slices were placed on a molybdenum pedestal which was heated from its underside by a pancake shaped heating coil. The pedestal was allowed to rotate in either a clockwise or counterclockwise motion by the pedestal

shaft. The carrier gas entered the bell jar assembly through the hollow pedestal shaft and was deflected downward onto the pedestal surface by the inner bell jar surface.

After the desired deposition was achieved, the bubbler was vented to air and the chamber temperature was reduced by shutting off the generator. The hydrogen flow was reduced to half a liter per minute and the system was allowed to purge and cool for twenty minutes. After the hydrogen purge, the system was opened to helium and purged for five minutes before opening the chamber to air and unloading.

If desired, it was possible to preclean the system using hydrogen chloride gas prior to deposition and after the high temperature hydrogen purge by opening valve C and allowing anhydrous hydrogen chloride to enter the carrier gas.

3.3 SUBSTRATE PREPARATION AND CLEANING

The silicon crystals used as substrates for the epitaxial process were grown by the Czochralski (83) technique by pulling a (111) oriented silicon seed from a silicon melt with a growth rate of 4 inches per hour and using a rotation rate of 25 RPM. Dislocation free crystals were prepared by the same method except that they were grown by the modified Czochralski techniques proposed by Dash (56). The crystal diameters were approximately 7/8 of an inch. The melt was doped with antimony and the final impurity concentrations in the crystals ranged from 1.5×10^{19} atoms/cm^3 to 2.5×10^{17} atoms/cm^3. This corresponds (84) to a resistivity range of 0.005 ohm·cm to 0.05 ohm·cm.

The crystallographic orientation of the sample was determined through the use of X-ray diffraction methods (85), and 50 mil thick slices were cut 1/2 to 1° off the (111) plane by a diamond blade. The slices were mechanically lapped using a 5 micron garnet abrasive lapping compound and then chemically polished in an HNO_3-HF-CH_3COOH-I_2 mixture until a final thickness of 35 mils was attained.

Substrates were examined for surface scratches and faults due to mechanical polishing, haze and orange peel caused by chemical polishing and for flatness through the use of interference fringes caused by optical flats placed over the surface (Plates 1 and 2).

Before epitaxial deposition, the slices were cleaned in HF for 15 seconds, rinsed in deionized water for 45 seconds, and then immersed in acetone until ready for use. Upon removal from the acetone, the slices were blown dry with nitrogen and placed in the chamber.

3.4 OBSERVATION OF IMPERFECTIONS IN SILICON FILMS

Imperfections in both the epitaxial deposit and substrate were observed through the use of preferential chemical etching agents. Dislocations were revealed by etching for four hours in a mixture of hydrofluoric, nitric and glacial acetic acids in the ratio of 1:3:10. This etch is commonly known as the Dash Etch (86).

Stacking faults were observed by etching for ten seconds in a mixture of hydrofluoric, nitric and glacial acetic acids in the ration of 3:5:3 saturated with Bromine. This etch is known as the CP-4 Etch and was developed by Vogel, Pfann, Corey and Thomas (87).

The presence of stacking faults was found to be observable without etching by using an interferometric microscope technique attributed to Nomarski and Weill (88). This technique is discussed in Appendix A.

Density measurements were made by counting etch pits in a 2 square millimeter area under 200 power magnification. Unless noted otherwise, the data is based on center readings.

3.5 RESULTS

3.5.1 DISLOCATIONS IN THE LAYER VS. DISLOCATIONS IN THE SUBSTRATE

In the first of a series of experiments, an epitaxial layer was deposited on five slices in the vertical deposition system. The layer thickness was evaluated by infra-red reflection interference techniques (Appendix B) and found to be approximately 9 microns. The slices were etched for the appearance of dislocations in the Dash Etch for times varying from 1 to 5 hours (Plate 3). Measurements of remaining layer thickness after one hour elapsed time intervals showed the etch rate to be approximately half a micron per hour. Etch pit counts were taken on each of the five samples, and the counts were plotted against etching time (Figure 2). It was noted that the count remained constant after a three hour etching time; this is characteristic of dislocation pits revealed by etching techniques. Based on the data obtained, a standard etching time of four hours was adopted.

The epitaxial slice that was etched for four hours was taken and the position of the pits marked on an optical comparator screen. The slice was suitably marked and then relapped until the layer was removed and the substrate revealed. The substrate was then repolished and re-etched to reveal dislocation pits in the bulk, and their position was overlaid on the comparator screen. The position of dislocation pits in the substrate and layer was then

evaluated. This method is similar to that of Light (44) and Chu and Gavaler (46) except that these authors note the position of the pits in the substrate before deposition. It was felt that the heat-treatment of the substrate during deposition might influence the presence of dislocations and, therefore, the experimental procedure was reversed.

The experimental overlay pattern obtained is shown in Figure 3. It is evident that very few dislocations are propagated into the deposited layer by growth from dislocations present in the substrate, while many dislocations are generated either at the interface or in the deposit.

3.5.2 STACKING FAULTS IN THE LAYER VS. DISLOCATIONS IN THE SUBSTRATE

A second set of five samples was deposited in the vertical system and etched for four seconds (Plate 4), two minutes (Plate 5), and then four minutes (Plate 6) in CP-4. It was noted that the size of the imperfections decreased with etching time (in opposition to a dislocation pit which normally increases once the fast etching planes have been revealed) and it was thus concluded that the imperfections were stacking faults. This is in agreement with the results of Dash (75).

The size of the fault edge was measured after the slices had been etched for four seconds and, using the relation given by Light (44), the calculated layer thickness was compared to the infra-red thickness measurements made before etching. The results are tabulated in Table I and are found to be in good agreement. These results are similar to those of Light and confirm the origination of the stacking faults to be at the epitaxial interface.

Previous to etching, the slices had been examined by Nomarski Interference contrast equipment (Plate 7). The fault size was found to be in excellent agreement with those of the etched samples. This method of observation may thus be used as a nondestructive means of measuring thickness and is of considerable value in estimating the qualitative presence of stacking faults.

The position of stacking faults was marked on an optical comparator screen and the sample was lapped back to the substrate, repolished and then re-etched in Dash Etch as in the previous section. An overlay was made to show stacking faults in the film superimposed on dislocations in the substrate. Figure 4 shows only a few stacking faults to be directly generated by dislocations in the substrate. It may be noted, however, that some stacking faults seem to be laterally offset from dislocations, as in the triad arrangements seen in the upper left corner of Figure 4. It is presumed that these stacking faults are associated with dislocations whose axes are not perpendicular to the growth plane.

3.5.3 STACKING FAULTS VS. GROWTH RATE

A series of deposition runs were made in the horizontal system which showed a relationship between growth rate and stacking fault density. In each run, five silicon slices were placed in line on the pedestal block situated at the center of the horizontal tube, and silicon was epitaxially deposited by flowing $SiCl_4$ into the tube from one end. In this horizontal chamber, the carrier gas is depleted of $SiCl_4$ as it passes from one end of the tube to the other and thus decreased the effective $SiCl_4$ concentration which in turn decreases the growth rate. Thus the thickness of the layers deposited in this system graded with distance along the tube length. The relation of stacking fault density to the effective growth rate produced by this variation is shown in Figure 5 for two horizontal runs and is seen to be linear.

Similar experiments have been performed with single slice vertical deposition runs and changes in the $SiCl_4$ - carrier gas mixture were made in order to change the growth rate; this resulted in the same relationship between growth rate and stacking fault density as observed in the horizontal system (Figure 5), but with a greater amount of spread due to variations in process parameters.

A variation of stacking fault density with radial distance was observed on almost all slices used for this experiment. Sample data comparing center readings and average edge values for stacking fault density are given for two vertical runs in Table II.

A definite sharp increase is noted in stacking fault density at the edge. It is assumed that the substrate edge provides a greater amount of surface area for heat absorption. The edge may thus provide a source of increased imperfection density cause by (1) a higher effective deposition temperature which, in turn, increases the effective growth rate or (2) by producing a high temperature gradient at the edge which produces an increase in stacking fault density per se.

A series of slices whose orientation was chosen to be within a few minutes of the (111) plane were grown at extremely slow growth rates of 0.1 micron per minute. In general, few surface defects or stacking faults were observed but, on a few slices, growth pyramids showing a growth step appearance were noted (Plate 8).

3.5.4 STACKING FAULT DENSITY VS. SUBSTRATE DISLOCATION DENSITY

In spite of the results found in Section 3.5.2 that stacking faults are not always propagated directly by dislocations, a relationship between fault density and substrate dislocation density has been noted.

A series of dislocation free substrates (Note 1) were placed in a horizontal deposition system whereby the slice positions alternated with other slices whose dislocation density was found to be approximately $3x10^3$ per square centimeter. For all other circumstances, the slices were exactly alike and were processed mechanically and chemically at the same time. The resultant stacking fault densities for the two series of substrates were determined as a function of chamber position and are shown in Figure 6. The dependence of density on position is related to the effective growth rate discussed in Section 3.5.3 and a relation of stacking fault density to dislocation is definitely seen. In all cases, the dislocation free substrates produced layers with greater stacking fault densities. Subsequent duplicate runs produced similar results.

- -

Note 1: Dislocation free material may be defined as material in which no dislocations appear parallel to the crystal growth axis and in which the dislocation loops are smaller than a given arbitrary size.

3.5.5 STACKING FAULTS VS. PREPARATION AND CLEANING PROCEDURES

The effects of substrate preparation and cleaning procedures on stacking fault density were investigated and were found to have a definite influence. Four runs were made in a vertical deposition system and the following points were investigated:

(1) The effect of mechanical polishing the substrate to an optical finish as compared with chemical polishing.

(2) The effect of cleaning slices in hydrogen prior to deposition.

(3) The effect of substrate cleaning in HCl immediately before deposition.

The results of these experiments are tabulated in Table 3 and it may be stated that, in general,

(1) Chemically polished slices produce layers with lower stacking fault densities than mechanical polished slices.

(2) Slices cleaned in hydrogen produce layers with lower stacking fault densities than slices which have not been cleaned.

(3) Substrates precleaned in HCl produce layers with lower stacking fault densities than those which have not been precleaned.

3.6 CONCLUSIONS AND DISCUSSION

The relation of dislocations in the epitaxial layer to those in the substrate and the relation of epitaxial stacking faults to substrate dislocations have been investigated by many authors (42,44,46) and the experimental results obtained in this investigation are in good agreement with work performed before. In general, the statements may be made that,

(1) Stacking faults and dislocations present in the layer are generally not directly propogated by imperfections in the substrate, and

(2) Stacking faults appear to be originated at the epitaxial interface.

Substrate handling and preparation were shown to have a significant effect on the stacking fault density. Increased surface perfection of the substrate slice, as indicated by lower stacking fault densities present on chemically polished substrates rather than mechanically polished substrates, is definitely desired. Also, the removal of surface or oxide films, as indicated by decreased stacking fault density layers in hydrogen baked or HCl cleaned substrates, seems to be good practice. These surface characteristics have been proposed by many (69,71,78) to be the major cause of stacking faults.

Because of the many proposals (69,71,78) and contradictions (79) brought forth, it seems that most of the mechanisms proposed

so far are sufficient for the production of stacking faults, but yet are not necessary conditions. The picture of epitaxial growth developed theoretically by Blisnakov (33) and Baur (34) and experimentally by Pashley (36) and Kurov (40) in which growth is initiated by random nuclei, extended by high surface atom migration rates, and propagated by the formation of new layers before the preceding layers have necessarily been completed, has recently been considered by Charig and Joyce (96) to be applicable to the silicon epitaxial system. Based on the experimental relationships between stacking fault density, substrate dislocation density and growth rate determined in this report, it is proposed that, for an epitaxial system as described by Charig and Joyce, the formation of stacking faults is controlled by the kinetics of the epitaxial process.

Jaccodine (97) has recently estimated the stacking fault energy of silicon to be less than 100 ergs/cm^2. He has thus proposed that the mechanism of stacking fault formation arises naturally from a collapsed vacancy cluster because the stacking fault should be the stable configuration in this low fault energy material.

The experimental results which indicate an increased stacking fault density with growth rate may be evaluated in the light of Jaccodine's (97) and Charig and Joyce's (96) proposals, and are seen to be in good agreement. As the deposition rate is increased, the surface nucleation rate is increased and a greater deviation

from an equilibrium growth condition occurs. This deviation creates a higher vacancy density because of the limited amount of surface migration of the epitaxial atoms and thus an increased number of vacancy clusters which are capable of collapsing into stacking faults.

The increased stacking fault densities observed on dislocation free substrates may also be explained by the same mechanism. The dislocation free surface provides no sites of easy nucleation for the epitaxial growth system. This lack of nucleation sites increases the surface vacancy density of the interface and creates a situation similar to that described before. This is confirmed by the reverse situation where extremely slow growth rates formed layers with few stacking faults but also produced pyramids which showed the presence of growth steps. In this case, epitaxial growth was accomplished by growth on only a few easy nuclei which then formed pyramids and by low surface vacancy saturations which then allowed the rate of atom migration to exceed the nucleation rate.

If the rate of atom migration becomes the controlling factor, then the atoms will migrate to easy nucleation sites, such as Frank screw dislocation sources. The layers formed by this type of growth might be expected to be free of stacking faults but show pyramids at points of easy nucleation, or growth steps at points on the surface where atom layers were allowed to grow by extension rather than by the simultaneous nucleation and growth of new layers.

4.0 APPENDIX A

INTERFERENCE CONTRAST MICROSCOPY

In 1955, Nomarski and Weill (88) developed an interferometric method for producing large variations in optical contrast for surfaces with height variations less than one order of interference. In this method, plane wave illumination is reflected from a surface with phase variations created by the surface profile. This wave is then passed through a double quartz prism and split into two coherent waves whose phase relation may be altered by adjustment of the double prism angle. These split waves are then recombined with a small lateral displacement at the microscope image plane, which results in the observation of an interference pattern between the two images. It should be noted that surfaces of constant slope would produce uniform intensities, while changes in slope would result in intensity variations. Because different slopes produce color changes which pass through the range of Newton interference colors, slope comparisons may be observed by color variations. Nomarski and Weill reported sensitivities of the order of 10Å when measuring the step heights of growth spirals in silicon carbide.

LeMehaute (89) reports the use of this method for observing (1) defects in evaporated metal films, (2) localized areas of ferrite and austenite phases in hardened Ni-Cr-Mo steels, (3) slip-line networks in cold-worked structures, (4) structural phase

changes produced by diffusion processes, and (5) substructures in sintered iron compacts. Eland (90) has applied the method to the study of corrosion patterns, and Jacquet (91) has attempted to use it as a tool for the observation of dislocations. The Nomarski Interference Contrast method has most recently been used by Dudley (92) as a means of observing stacking faults in epitaxial silicon layers.

5.0 APPENDIX B

INFRA-RED INTERFERENCE THICKNESS MEASUREMENT

Spitzer and Tannenbaum (93) have proposed that the interface between the substrate and deposit of an epitaxial growth system might act as a reflecting surface to infra-red light if the doping impurity levels of the deposit was significantly different from that of the substrate and thus affect the index of refraction; through the use of reflectance interference fringes, the thickness could then be measured. Extensive revision and modification of this method has been made by Albert and Combs (94).

If an incident beam of light, 1, (Figure 7) strikes the surface of the epitaxial film at an angle I from the normal, part of this beam is reflected at the epitaxial layer surface as beam 2. The remainder is refracted by the film layer, passes through the film, is reflected at the epitaxial interface and finally emerges from the layer as beam 3. The combined intensity of the net reflected ray at a given wavelength is a function of the phase difference between the two reflected rays. For constructive interference to occur, it can be shown that the thickness of the film and the wavelength must be related by:

$$2t\mu \cos I' = M\lambda$$

Where t = thickness of film

I' = internal reflectance angle

μ = index of refraction

M = any positive integer

λ = wavelength of light

Since M may be any whole number, there will be a series of values of λ for which constructive interference will occur, and although M cannot be determined, the difference between any two integer values may be easily found. Thus, for constructive interference at wavelength λ,

$$2t\mu \cos I' = M_1 \lambda_1$$

and at any other maximum, i.e., λ_2,

$$2t\mu \cos I' = M_2 \lambda_2$$

The difference $M_1 - M_2$ is just the number of maxima between λ_1, and λ_2 and may be written as:

$$M_1 - M_2 = n = \frac{2t\mu \cos I'}{\lambda_1} - \frac{2t\mu \cos I'}{\lambda_2} = 2t\mu \cos I' \left(\frac{1}{\lambda_1} - \frac{1}{\lambda_2} \right),$$

and solving for t, we obtain:

$$t = \frac{n}{2\mu \cos I'} \left(\frac{\lambda_1 \lambda_2}{\lambda_2 - \lambda_1} \right)$$

A graphic representation of per cent transmission versus wavelength would thus provide an interference type curve from which consecutive maxima may be chosen to calculate thickness. The Beckman IR-5A reflectance attachment has an incident angle of $I = 30°$ and, if the index of refraction for silicon (95) is taken as $\mu = 3.42$, then by Snells Law we may find $I' = 8.4°$ or $\cos I' \doteq .99 \approx 1$. The thickness of an epitaxial silicon layer may thus be calculated from any two consecutive maxima ($n = 1$) according to the equation:

$$t = \frac{\lambda_1 \lambda_2}{6.84 (\lambda_2 - \lambda_1)}$$

6.0 BIBLIOGRAPHY

1. Gibbs, J. W., Collected Works, Longmans, Green and Co., (1928).
2. Curie, P., Bull. Soc. Min. DeFrance, 8, 145 (1885).
3. Wulff, G.,Z. Krist, 34, 449 (1901).
4. Hilton, H., Mathematical Crystallography, Oxford (1903).
5. Herring, C., Phys. Rev., 82, 87 (1951).
   Herring, C., Solid Surfaces, Univ. Chicago Press (1953), p. 5.
6. Frank, F. C., Growth and Perfection of Crystals, Wiley (1958), p.3.
7. Batterman, B. W., J. A. P., 28, 1236 (1957).
8. Jaccodine, R. J., J.A.P., 33, 2643 (1962).
9. Gibbs, J. W., Collected Works, Longmans, Green and Co., (1928) Vol. 1, p. 325 footnote.
10. Buckley, H. E., Crystal Growth, Wiley (1951).
11. Becker, R., and Doring, W., Ann. Physik, 24, 719 (1935).
12. Volmer, M., Kinetik der Phasenbildung, Dresden and Leipzig: Steinkopff (1939).
13. Haward, R. N., Trans. Far. Soc., 35, 1401 (1939).
14. Volmer, M., and Schultz, W., Z. Phys. Chem., A156, 1 (1931).
15. Frank, F. C., Proc. Phys. Soc., A62, 131 (1949).
    Frank, F. C., Disc. Far. Soc., 5, 48-67 (1949).
    Frank, F. C., Disc. Far. Soc., 5, 186 (1949).
    Frank, F. C., Phil. Mag., 42, 1014 (1951).
    Frank, F. C., Adv. Phys., 1, 91 (1952).
16. Burton, W. K., and Cabrera, N., Disc. Far. Soc., 5, 33-40 (1949).
17. Burton, W. K., Cabrera, N., Frank, W. C., Nature 163, 398 (1949).
    Burton, W. K., Cabrera, N., Frank, W. C., Phil. Trans. Roy. Soc., A243, 299 (1951).
18. Amelinckx, S., Phil. Mag., Ser. 7, 43, 562 (1952).
19. Forty, A. J., Phil. Mag., Ser. 7, 43, 481 (1952).
    Forty, A. J., Phil. Mag., Ser. 7, 42, 670 (1951).
20. Griffin, L. J., Phil. Mag., Ser. 7, 41, 196 (1950).
21. Dawson, I. M., Vand, V., Nature, 167, 476 (1951).
22. Verma, A. R., Amelinckx, S., Nature, 167, 939 (1951).
23. Cahn, J. W., Acta Met., 8, 554 (1960).
24. Nabarro, F. R. N., Jackson, P. J., Growth and Perfection of Crystals, Wiley (1958), p. 11.
25. Cabrera, N., and Coleman, R. V., ASTIA Report No. AD276403, (1962).
26. Van Arkel, A. E., Physica, 61, 316 (1925).
27. Royer, L., Bull. Soc. France. Mineral., 51, 7 (1928).
28. Lassen, H., Brueck, L., Ann. Physik, 22, 65 (1935).
29. Frank, F. C., Van Der Merwe, J. H., Proc. Roy. Soc. (London), A198, 205 (1949).
30. Blackman, M., Proc. Phys. Soc., A65, 1040 (1952).
31. Pashley, D. W., Adv. Phys., 5, 173 (1956).

32. Deo, A. E., Finch, G. I., Gharpurey, M. K., Proc. Roy. Soc. (London), A236, 7 (1956).
33. Blisnakov, G., Compt. Rend., 242, 656 (1956).
34. Baur, E., Z. Krist., 110, 372 (1958).
35. Dixit, K. R., Proc. Indian Acad, Sci., A48, 330 (1958).
36. Pashley, D. W., Epitaxy in Thin Surface Films, AIME Advanced Electronics Materials Conference, Philadelphia, Penna., August 28, 1962.
37. Marinace, J. C., IBM Journal, 4, 248 (1960).
38. Theuerer, H. C., J. Electrochem. Soc., 108, 649 (1961).
39. Theuerer, H. C., Kleimak, J. J., Loar, H. H., Christensen, H., Proc. I.R.E., 48, 1642 (1960).
40. Kurov, G. A., Fizika Tverdogo Tela, 3, 1662 (1961).
Kurov, G. A., Fizika Tverdogo Tela, 4, 564 (1962).
41. Vermout, P., and Dekeyser, W., Physica, 25, 53 (1959).
42. Ingham, H. S. Jr., McDade, P. J., IBM Jour., 4, 302 (1960).
43. Ingham, H. S. Jr., McDade, P. J., Compton, D. M. J., AIME Conf., 12, 285 (1961).
44. Light, T. B., AIME Conf., 15, 137 (1962).
45. Reizman, F., Basseches, H., AIME Conf., 15, 169 (1962).
46. Chu, T. L., and Gavaler, J. R., AIME Conf., 19, 209 (1963).
47. Flint, P. S., Lawrence, J. E., and Tucker, R., Electrochem. Soc. Conf., Silicon Epitaxial (111) Surface Defects, Abstract No. 73, Los Angeles, Calif. (1963).
48. Tung, S. K., The Effects of Substrate Orientation on Epitaxial Silicon Growth, Electrochem. Society Meeting, New York, Oct. 31, 1963.
49. Edmunds, G. H., Gibson, W. C., Bell Telephone Laboratories, Private Communication.
50. Sterling, E., Bell Telephone Laboratories, Private Communication.
51. Cottrell, A. H., Dislocations and Plastic Flow in Crystals, Oxford (1953).
52. Read, W. T., Jr., Dislocations in Crystals, McGraw-Hill (1953).
53. VanBueren, H. G., Imperfections in Crystals, North-Holland (1961).
54. Beatty, H. J., Glang, R., Kren, J. G., ASTIA Report No. AD-259-477 (1962).
55. Glang, R., Wajda, E. S., AIME Conf., 15, 27 (1962).
56. Dash, W. C., Growth and Perfection of Crystals, Wiley (1958), p. 361.
57. Queisser, H. J., J. A. P., 32, 1776 (1961).
58. Seeger, A., Defects in Crystalline Solids, Phys. Soc., London, (1955), p. 328.
59. Heidenreich, A. D., and Shockley, W., Strength of Solids (London: Phys. Soc.) (1948), p. 57.
60. Fullman, R., J.A.P., 22, 448 (1951).
61. Seeger, A., Schoeck, G., Acta Met., 1, 519 (1953).
62. Schoeck, G., Seeger, A., Defects in Crystalline Solids, Phys. Soc. London (1955), p. 340.
63. Hirsch, P. B., Silcox, J., Growth and Perfection of Crystals, Wiley (1958), p. 262.

64. Silcox, J., Hirsch, P. B., Phil. Mag., 4. 72 (1959).
65. Kuhlman-Wilsdorf, D., Phil. Mag., 3, 125 (1958).
66. Nakayama, Y., Weissmann, S., Imura, T., Direct Observation of Imperfections in Crystals, Wiley (1962), p. 573.
67. Howie, A., Direct Observation of Imperfections in Crystals, Wiley (1962), p. 269.
68. Sloope, B. W., and Tiller, C. O., J.A.P., 32, 1331 (1961).
69. Schwuttke, G. H., J.A.P., 33, 1538 (1962).
70. Schwuttke, G. H., Sils, V., Electrochem. Soc. Mtg., Paper No. 82, Los Angeles, Calif. (1962).
71. Queisser, H. J., Finch, R. H., Washburn, J., J.A.P., 33, 1536, (1962).
72. Booker, G. R., Stickler, R., J.A.P., 33, 3281 (1962).
73. Wynne, R. H., and Goldberg, C., Trans. AIME, 197, 436 (1953).
74. Lenie, C. A., Electrochem. Soc. Mtg., Paper No. 73, Los Angeles, Calif. (1962).
75. Dash, W. C., J.A.P., 33, 2395 (1962).
76. Lang, A. R., J.A.P., 29, 597, (1958).
    Lang, A. R., J.A.P., 30, 1748 (1959).
77. Haase, O., AIME Conf., 15, 159 (1962).
78. Finch, R. H., Queisser, H. J., Thomas, G., Washburn, J., J.A.P., 34, 406 (1963).
79. Batsford, K.O., Thomas, D. J. D., Solid State Electronics, 5, 353 (1962).
80. Theuerer, H. C., Bell Laboratories Record, 33, 327 (1955).
81. Allegretti, J. E., Pollak, P. I., Materials Science and Technology for Advanced Applications, Prentice-Hall (1962), p. 498.
82. Handbook of Chemistry and Physics, 36th Edition, Chemical Rubber Publishing Co. (1954).
83. Czochralski, Z. Physik, Chem., 92, 219 (1917).
84. Irvin, J. C., B.S.T.J., 41, 287 (1962).
85. Wood, A., Crystal Orientation Manual, Columbia Univ. Press (1963).
86. Dash, W. C., J.A.P., 27, 1193 (1956).
87. Vogel, F. L., Pfann, W. G., Corey, H. E., Thomas, E. E., Phys. Rev., 90, 489 (1953).
88. Nomarski, G., Weill, A. R., 52, 121 (1955).
89. Le Mehaute, C., IBM Jour., 6, 263 (1962).
90. Eland, A. J., Philips Tech. Rev., 22, 228 (1960).
91. Jacquet, P., C. R. Acad. Sci., 253, 1328 (1961).
92. Dudley, R. H., Bell Telephone Laboratories, Private Communication.
93. Spitzer, W. G., Tannenbaum, M., J.A.P., 32, 744 (1961).
94. Albert, M. P., Combs, J. F., Electrochem. Soc. Mtg., Detroit, Mich., (1961).
95. Ballard, S. S., Univ. Mich. Willow Run Lab. Rept. No. 2389-11-S, (1959).
96. Charig, J. M., Joyce, B. A., J. Electrochem. Soc., 109, 957 (1962).
97. Jaccodine, R. J., App. Phys. Letters, 2, 201 (1963).

7.0 FIGURES

FIGURE 1

DIAGRAMATIC ILLUSTRATION OF THE EXPERIMENTAL

EPITAXIAL DEPOSITION SYSTEM

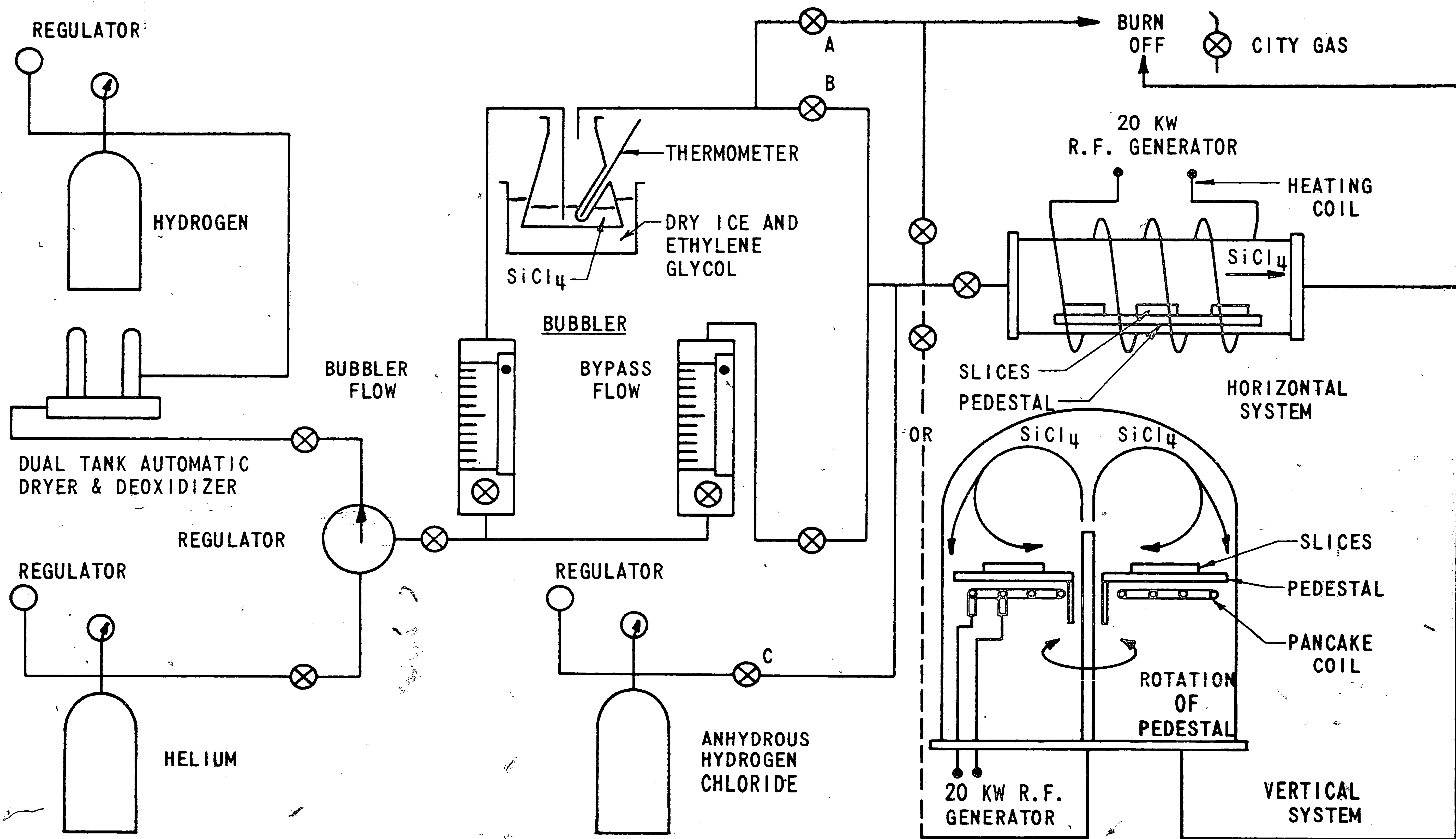

REGULATOR
HYDROGEN
DUAL TANK AUTOMATIC
DRYER & DEOXIDIZER
REGULATOR
REGULATOR
HELIUM
BUBBLER
FLOW
THERMOMETER
DRY ICE AND
ETHYLENE
GLYCOL
SiCl4
BUBBLER
BYPASS
FLOW
REGULATOR
ANHYDROUS
HYDROGEN
CHLORIDE
A
B
C
BURN
OFF
CITY GAS
20 KW
R.F. GENERATOR
HEATING
COIL
SiCl4
SLICES
PEDESTAL
HORIZONTAL
SYSTEM
OR
SiCl4
SiCl4
SLICES
PEDESTAL
PANCAKE
COIL
ROTATION
OF
PEDESTAL
20 KW R.F.
GENERATOR
VERTICAL
SYSTEM

FIGURE 2

RELATIONSHIP BETWEEN TIME AND PIT DENSITY FOR SILICON EPITAXIAL LAYERS ETCHED IN DASH ETCH

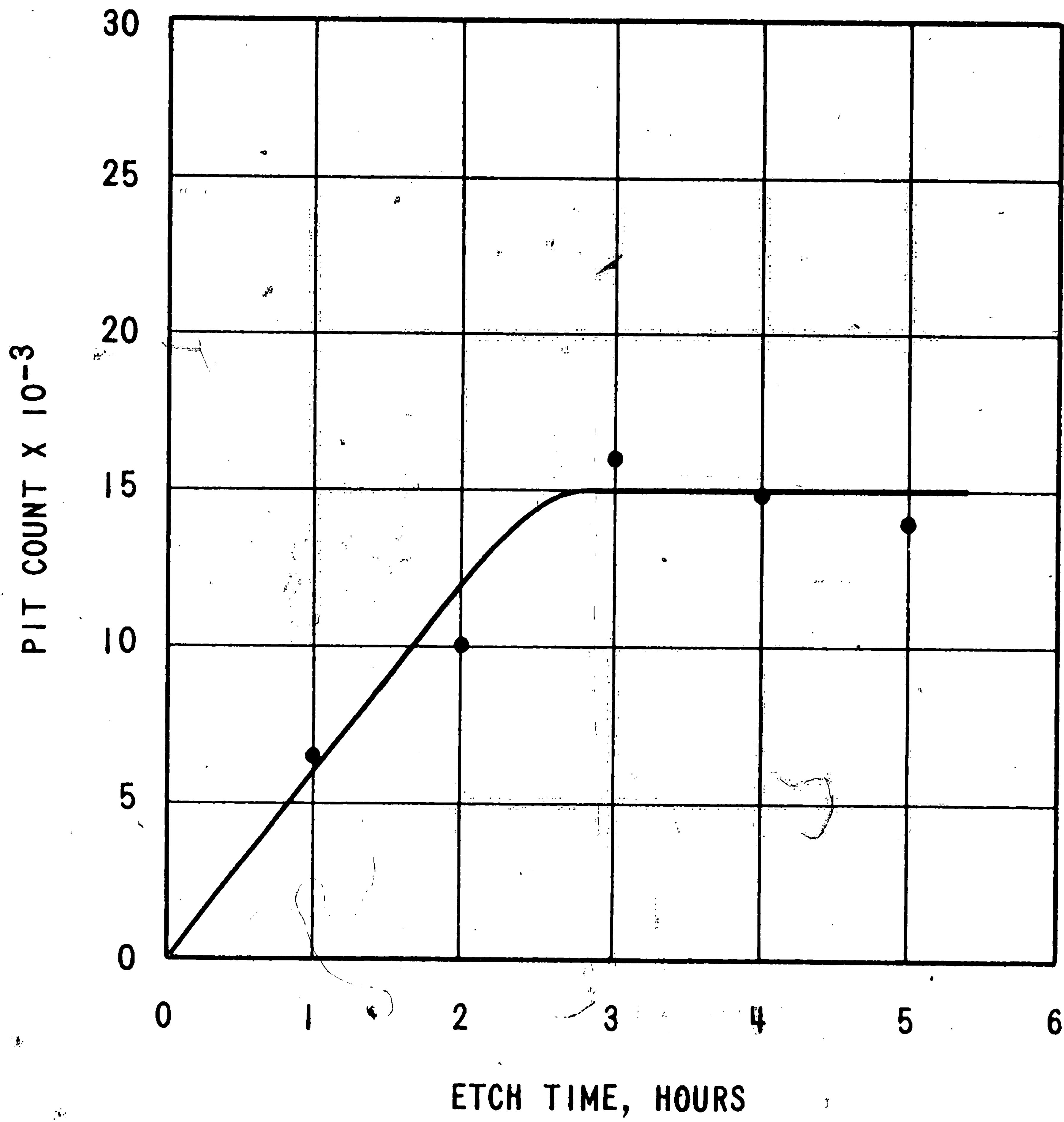
30
25
20
15
10
5
0
PIT COUNT X 10^{-3}
0
1
2
3
4
5
6
ETCH TIME, HOURS

FIGURE 3

OVERLAY PATTERN SHOWING THE RELATION OF
DISLOCATION PITS IN THE SUBSTRATE TO
DISLOCATION PITS IN THE LAYER

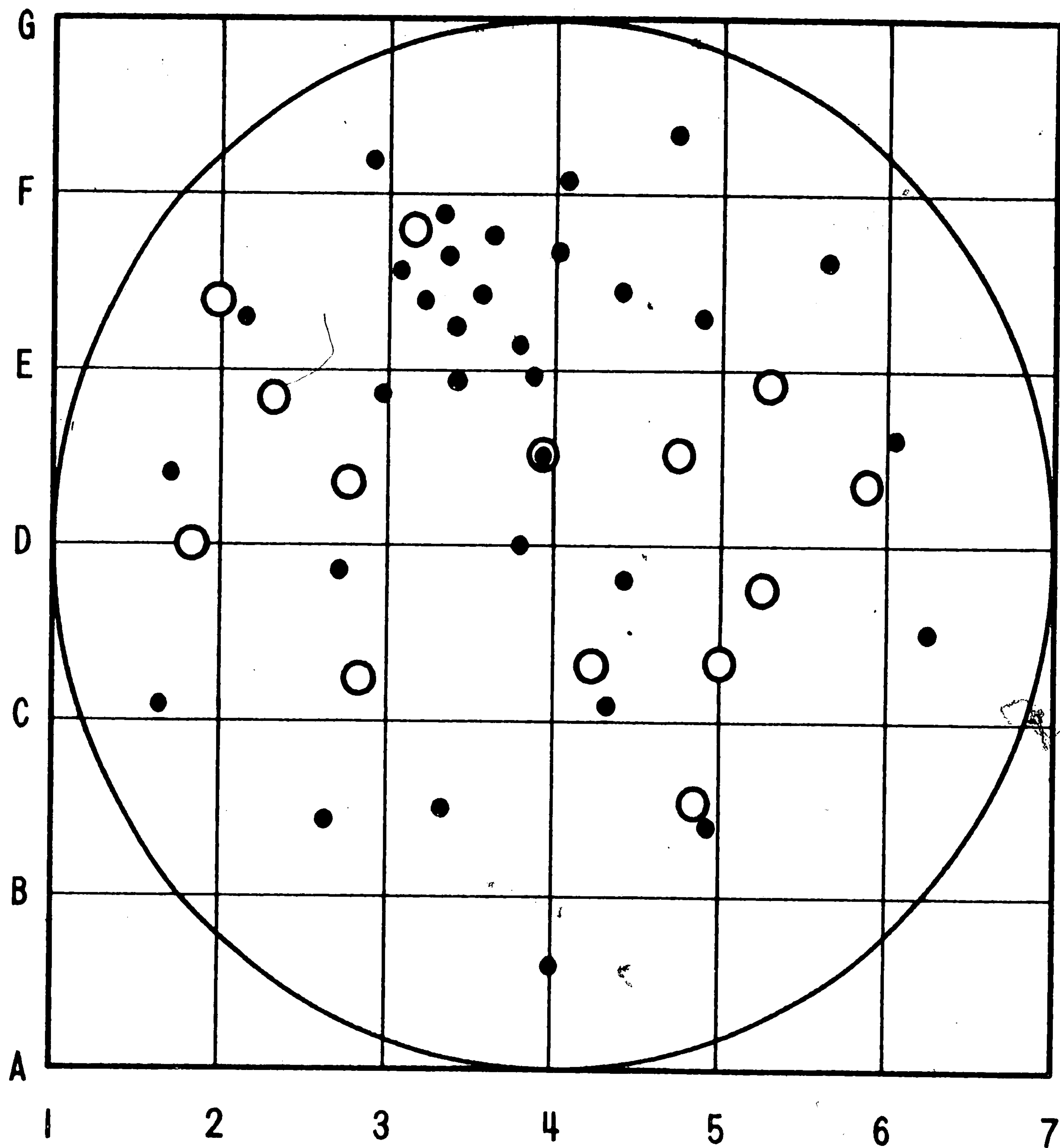
G
F
E
D
C
B
A
1
2
3
4
5
6
7
EPITAXIAL LAYER
SUBSTRATE

FIGURE 4

OVERLAY PATTERN SHOWING THE RELATION OF
DISLOCATION PITS IN THE SUBSTRATE TO
STACKING FAULTS IN THE LAYER

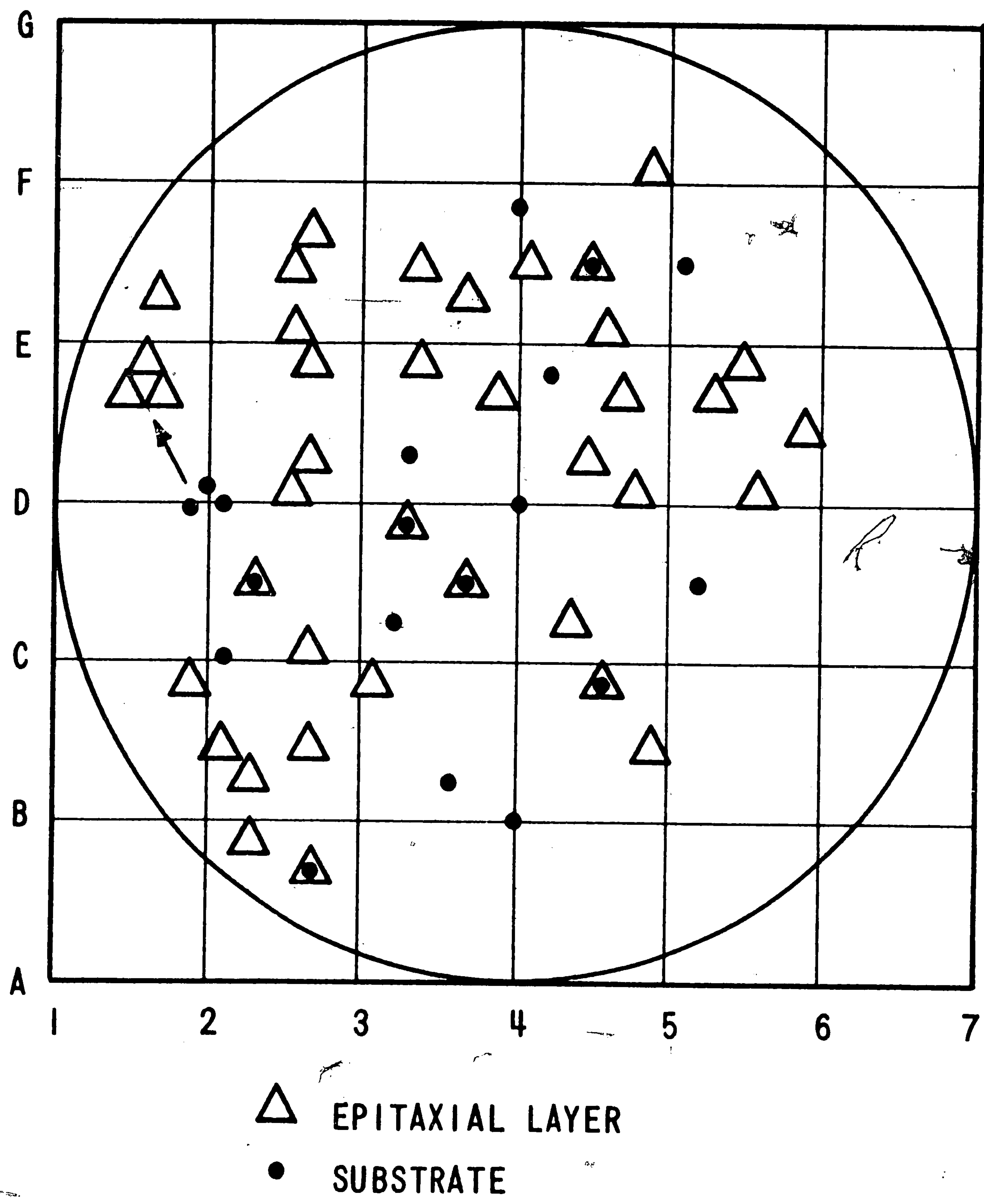
G
F
E
D
C
B
A
1
2
3
4
5
6
7
EPITAXIAL LAYER
SUBSTRATE

FIGURE 5

RELATIONSHIP BETWEEN GROWTH RATE AND

STACKING FAULT DENSITY

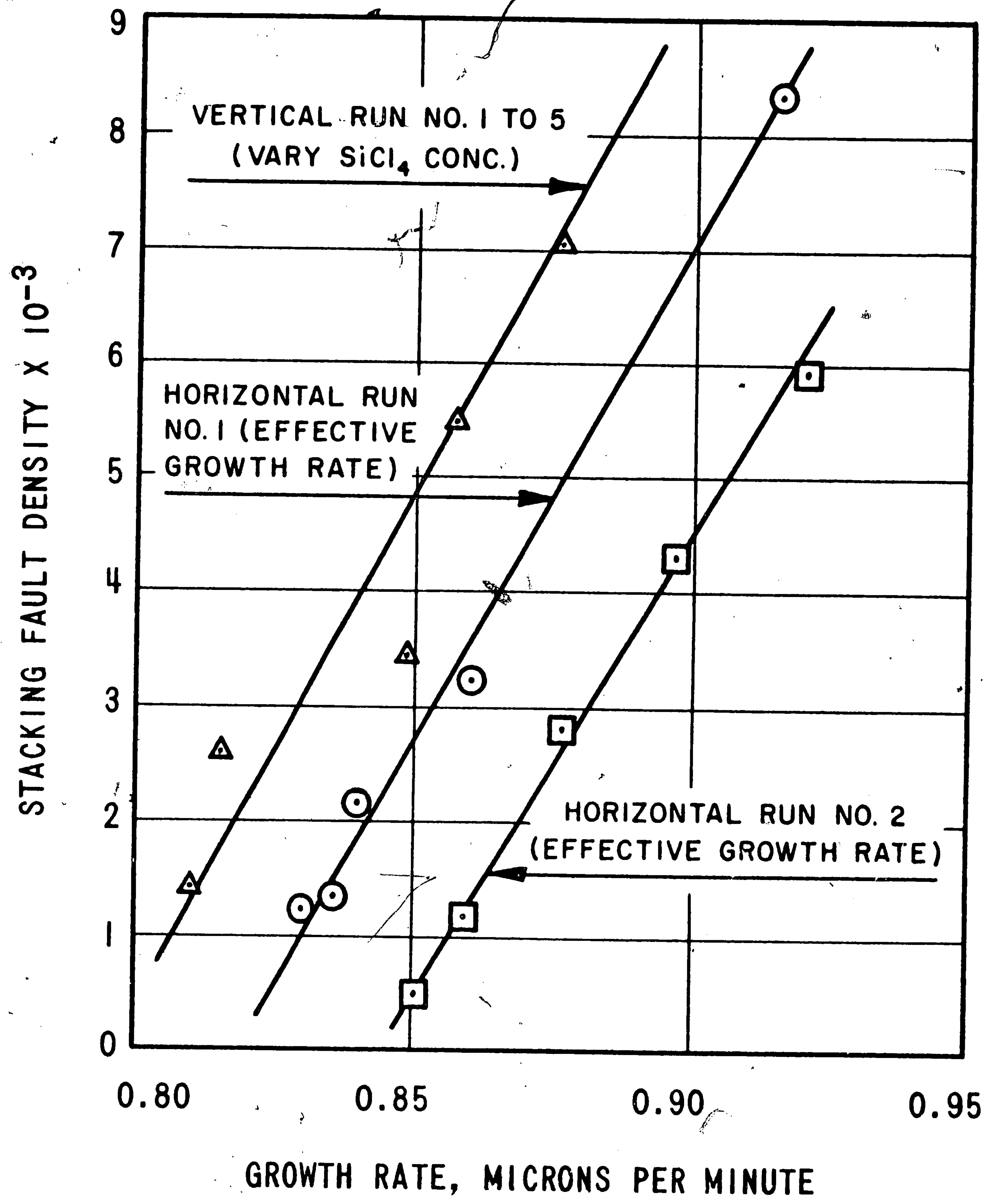

STACKING FAULT DENSITY X 10^{-3}
GROWTH RATE, MICRONS PER MINUTE
0.80
0.85
0.90
0.95
0
1
2
3
4
5
6
7
8
9
VERTICAL RUN NO. 1 TO 5
(VARY $SiCl_4$ CONC.)
HORIZONTAL RUN
NO. 1 (EFFECTIVE
GROWTH RATE)
HORIZONTAL RUN NO. 2
(EFFECTIVE GROWTH RATE)

FIGURE 6

RELATIONSHIP BETWEEN SUBSTRATE DISLOCATION DENSITY
AND STACKING FAULT DENSITY IN THE LAYER

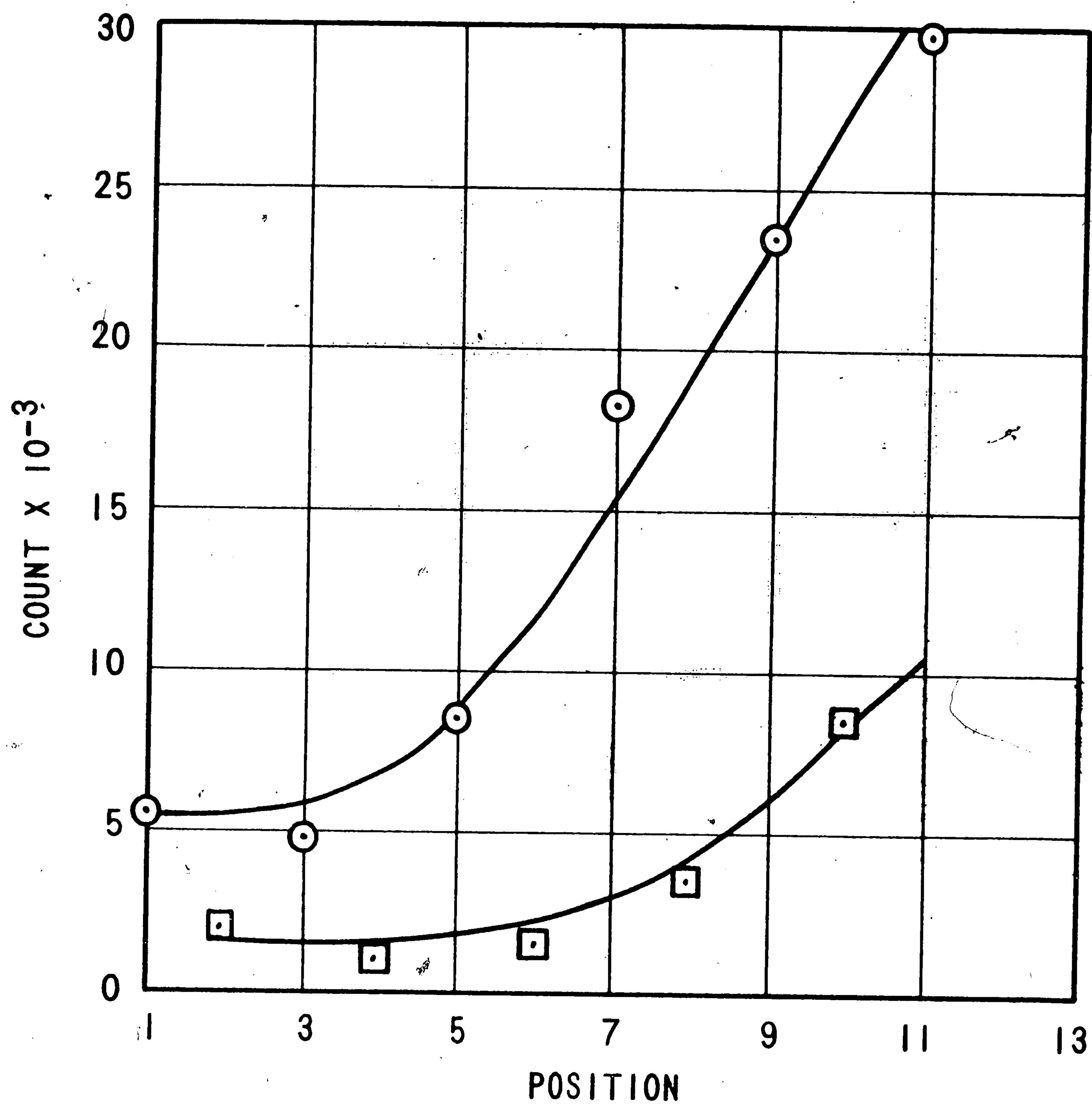
30
25
20
15
10
5
0
COUNT X 10^{-3}
1
3
5
7
9
11
13
POSITION
DISLOCATION FREE SUBSTRATE
3.2 X 10^3 DISLOCATION SUBSTRATE

FIGURE 7

RELATIONSHIP BETWEEN INCIDENT AND REFLECTED BEAMS FOR THE INFRARED MEASUREMENT OF EPITAXIAL THICKNESS

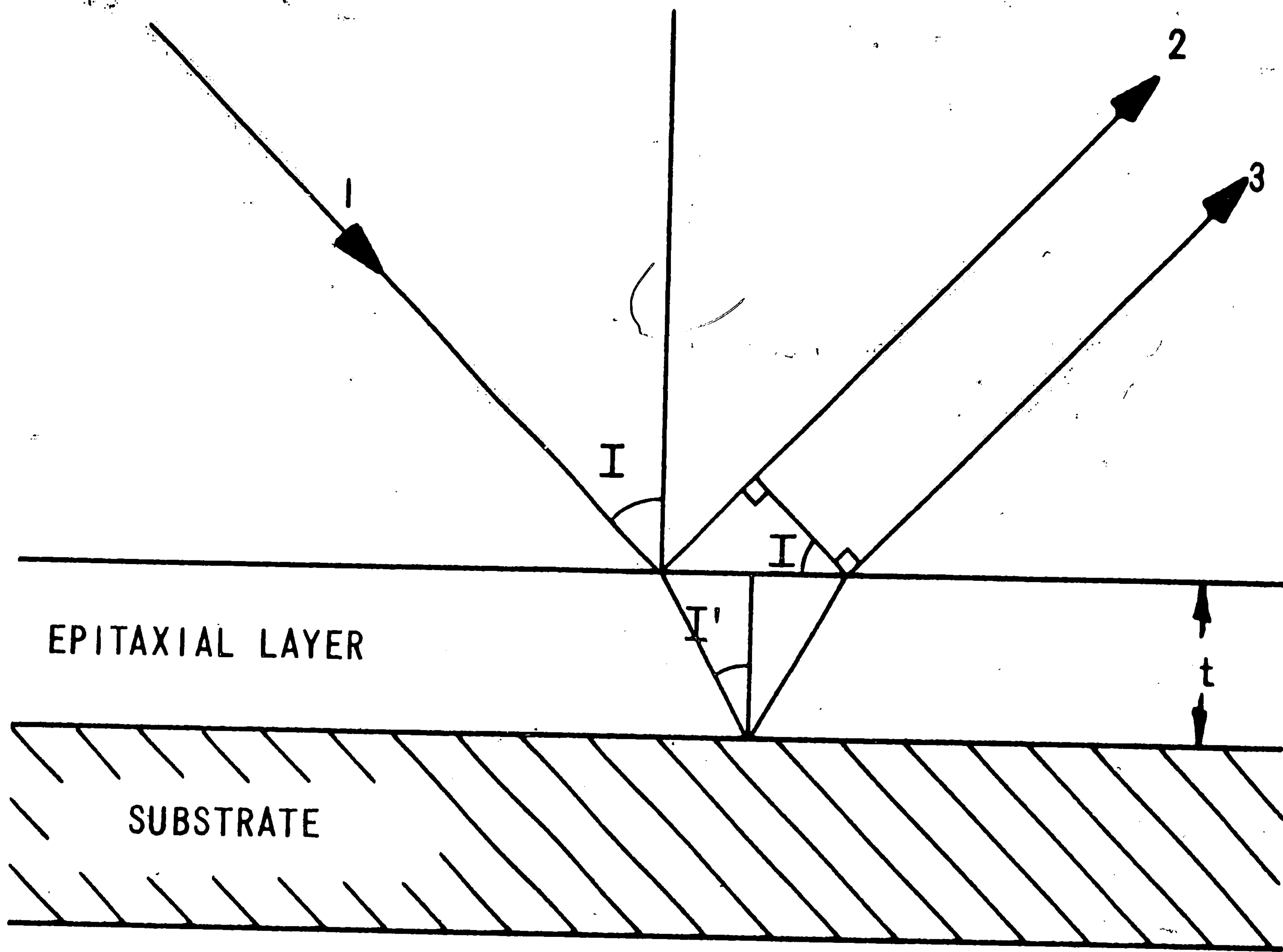
1
2
3
I
I
I'
t
EPITAXIAL LAYER
SUBSTRATE

8.0 PLATES

PLATE 1

INTERFERENCE FRINGES ON A FLAT EPITAXIAL DEPOSIT

200x

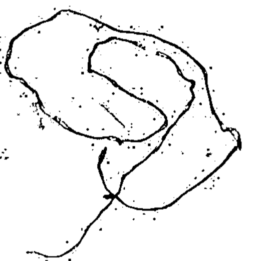

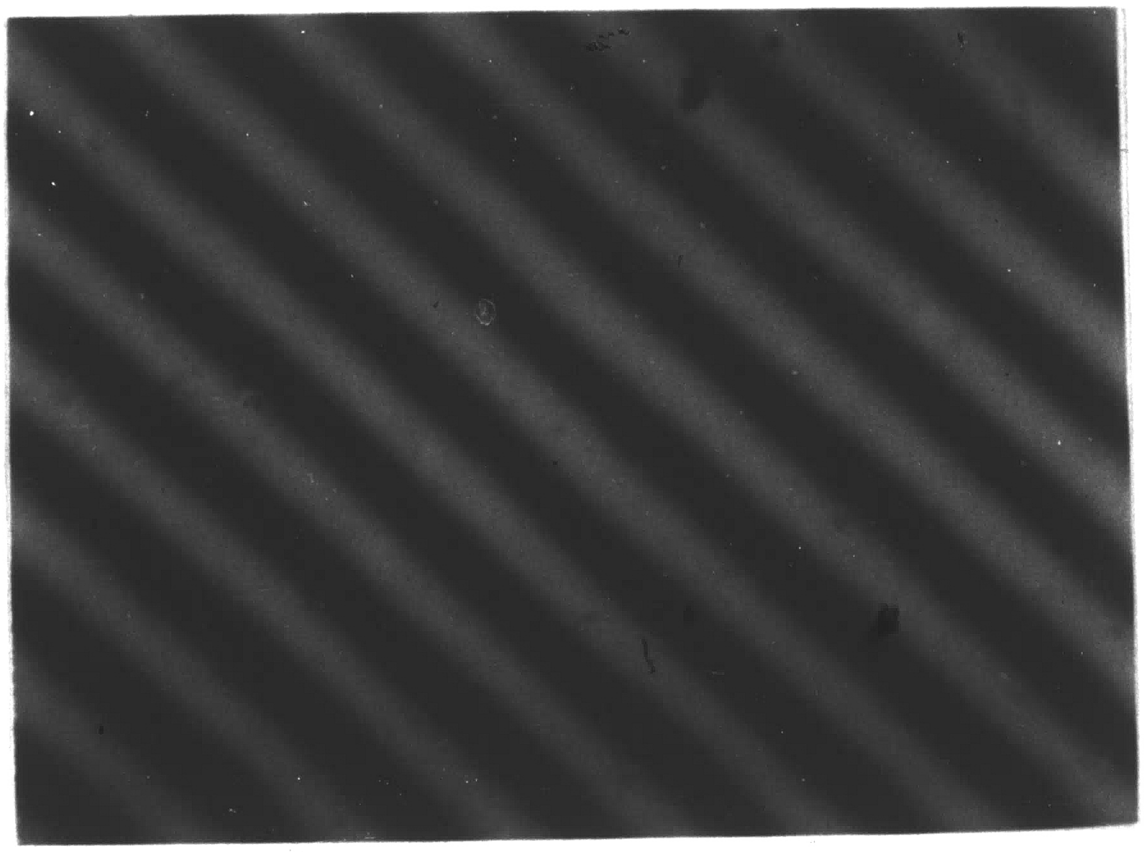

PLATE 2

INTERFERENCE FRINGES ON AN EPITAXIAL LAYER

SHOWING PITTING

200x

PLATE 3

ETCH PITS IN EPITAXIAL SILICON LAYERS ETCHED

IN DASH ETCH FOR 4 HOURS

500x

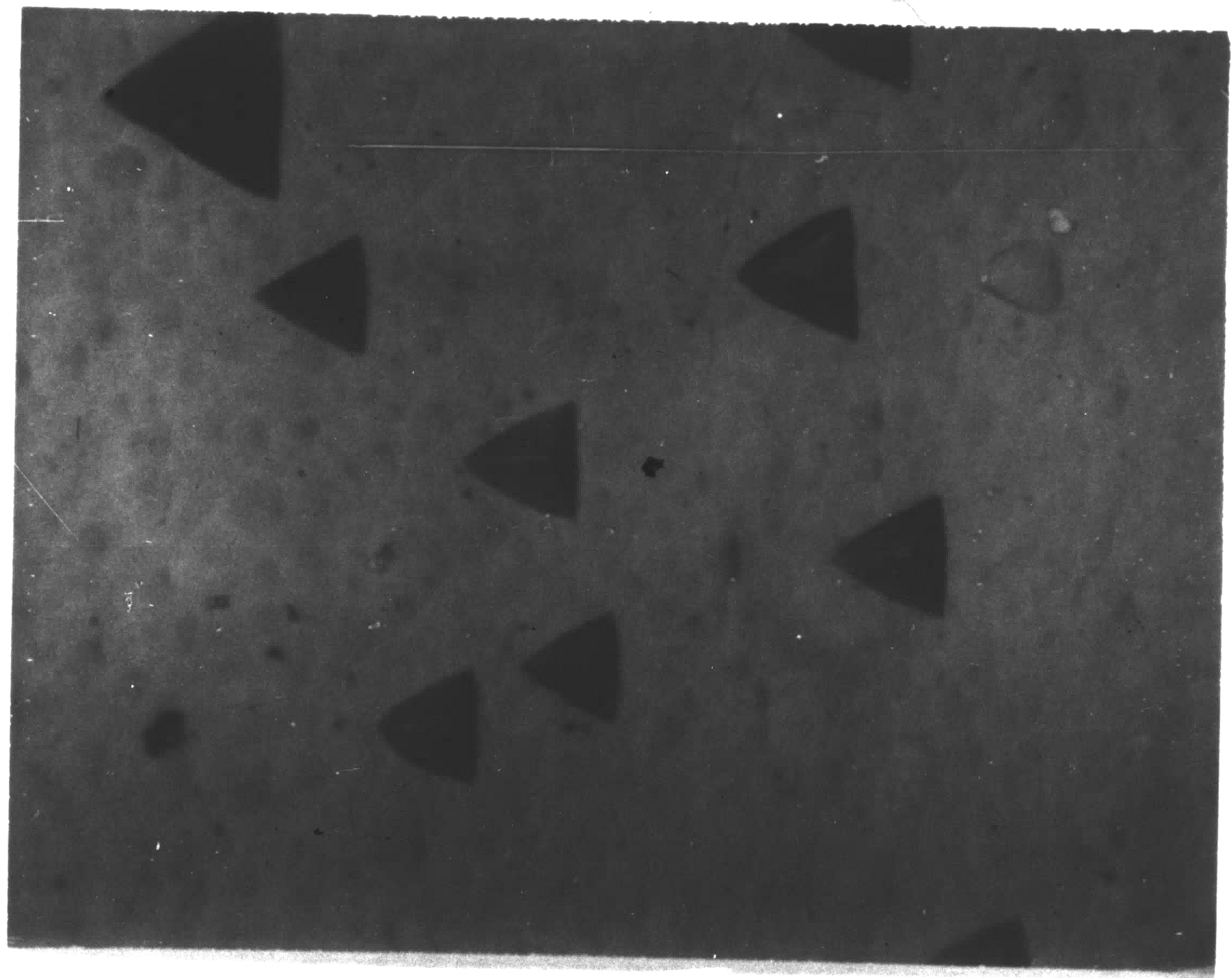

PLATE 4

STACKING FAULTS IN EPITAXIAL SILICON LAYER

ETCHED IN CP-4 FOR 4 SECONDS

200x

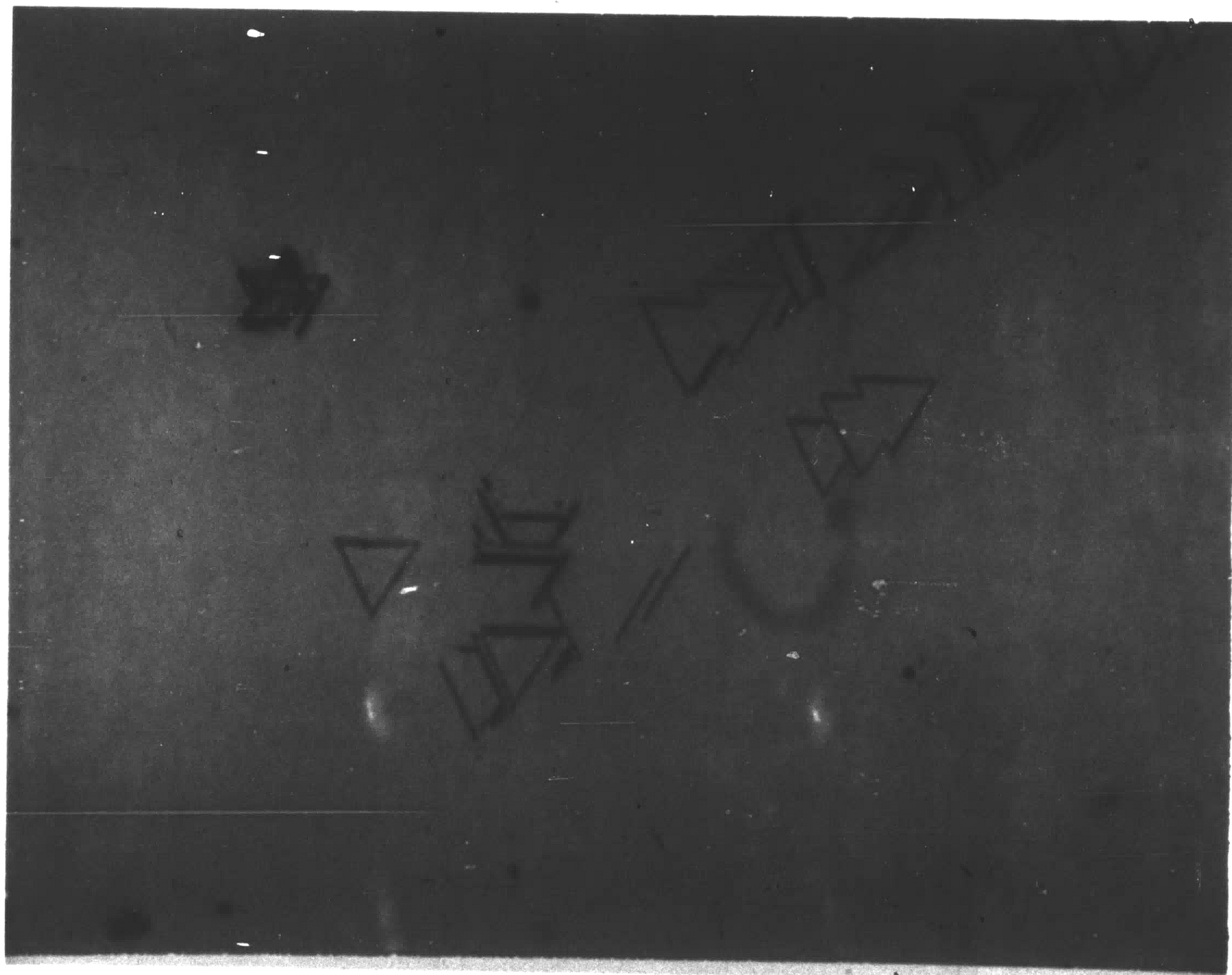

PLATE 5

STACKING FAULTS IN EPITAXIAL SILICON LAYER

ETCHED IN CP-4 FOR 2 MINUTES

200x

PLATE 6

STACKING FAULTS IN EPITAXIAL SILICON LAYER

ETCHED IN CP-4 FOR 4 MINUTES

200x

PLATE 7

STACKING FAULT IN EPITAXIAL SILICON OBSERVED

BY INTERFERENCE CONTRAST MICROSCOPY

200x

PLATE 8

GROWTH PYRAMID SHOWING STEPS ON EPITAXIAL SILICON

LAYER GROWN AT 0.1 MICRON PER MINUTE

1000x

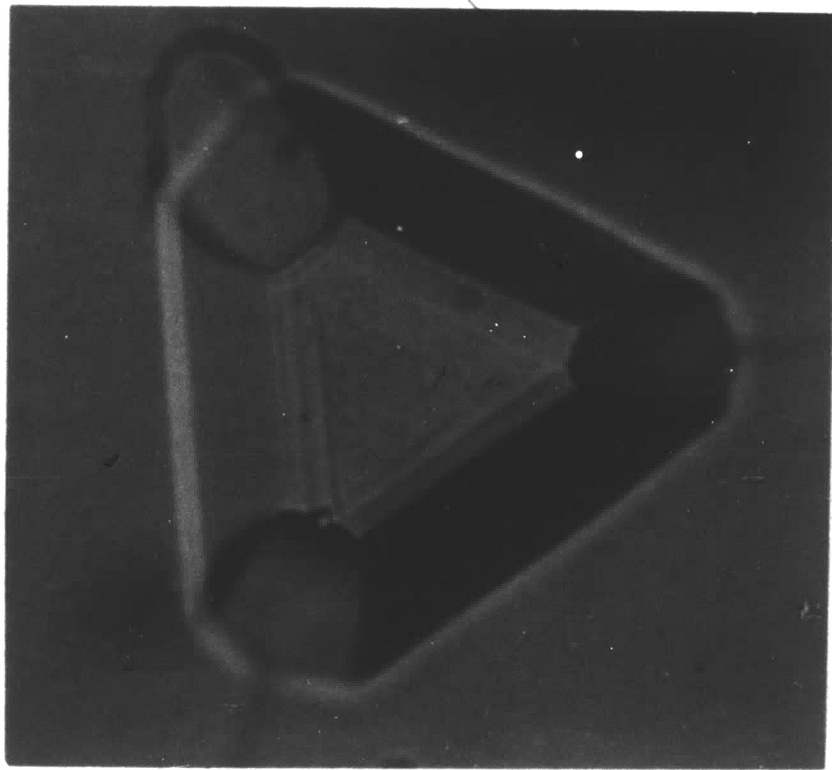

9.0 TABLES

TABLE 1

Comparison of Layer Thickness Values Calculated

From Fault Edge and Infrared Techniques

Slice No.	Fault Size, mm.	Fault Edge Layer Thickness, microns	Infrared Layer Thickness, microns
EA297-6	0.0110	8.95	8.9
EA297-7	0.0100	8.15	8.2
EA297-8	0.0100	8.15	8.3
EA297-9	0.0088	7.20	7.4
EA297-10	0.0088	7.20	7.0

TABLE 2

RADIAL VARIATION OF STACKING FAULT DENSITY

Slice No.	Center Fault Density, cm^{-2}	Edge Fault Density, cm^{-2}
EA764-1	0	2.1×10^2
EA764-2	1.6×10^3	4.8×10^3
EA764-3	0	1.1×10^2
EA764-4	3.0×10^3	2.9×10^3
EA765-1	0	80
EA765-2	0	4.4×10^3
EA765-3	0	1.9×10^2

TABLE 3

COMPARISON OF PREPARATION TECHNIQUES

ON STACKING FAULT DENSITY

	Density, cm^{-2}			
Slice No.	Run No. 1 Mechanical Polish	Run No. 2 Chemical Polish	Run No. 3 Chemical Polish & Hydrogen Bake	Run No. 4 Chemical Polish, Hydrogen Bake, HCl Preclean
1	10^6	5.1×10^4	8.0×10^3	2.5×10^2
2	10^6	8.8×10^4	5.1×10^4	3.6×10^3
3	5.8×10^5	1.2×10^3	5.9×10^4	1.2×10^3
4	10^6	10^6	3.2×10^4	8.3×10^3
5	4.1×10^4	6.0×10^4	7.2×10^3	8.1×10^3

10.0 BIOGRAPHY

Michael R. Notis was born on August 6, 1938, in Brooklyn, New York. After Mr. Notis was graduated from Far Rockaway High School, he attended Lehigh University on a scholarship from Grumman Aircraft Engineering Company, receiving a Bachelor of Science Degree in Metallurgical Engineering in 1960.

Since June 1960, Mr. Notis has been employed by the Western Electric Company in Allentown, Pennsylvania. He has participated in the Western Electric Development Engineering Program and, while on assignment to the Bell Telephone Laboratories, authored a paper entitled "Decarburization of Iron-Nickel-Cobalt Glass-Sealing Alloys" which was published in the Journal of the American Ceramic Society. In 1962, while a member of the Metallurgical Development Engineering organization of Western Electric, he worked with the heat-treatment of metals for solid state devices and the evaluation of epitaxial semiconductor deposits. Mr. Notis is now concerned with the development of solid state integrated circuit logic devices.